

Bugs on a Circle

Josh Briley & Bryan Quaife

Abstract

We describe and analyze a generalization of the classic “Four Bugs on a Square” cyclic pursuit problem. Instead of allowing the bugs to spiral towards one another, we constrain N bugs to the perimeter of the unit circle. Depending on their configuration, each bug moves either clockwise or counterclockwise with a constant angular speed, or remains stationary. Unlike the original problem where bugs always coalesce, this generalization produces three possible steady states: all bugs coalescing to a single point, clusters of bugs located at two antipodal points, or bugs entering a stable infinite chase cycle where they never meet. We analyze the stability of these steady states and calculate the probability that randomly initialized bugs reach each state. For $N \leq 4$, we derive exact analytical expressions for these probabilities. For larger values, we employ Monte Carlo simulations to estimate the probability of coalescing, finding it approximately follows an inverse square root relationship with the number of bugs. This generalization reveals rich dynamical behaviors that are absent in the classic problem. Our analysis provides insight into how restricting the bugs to the circle’s perimeter fundamentally alters the long-term behavior of pursuing agents compared to unrestricted pursuit problems.

1 Introduction

In the classic four bugs on a square problem, four bugs are initially placed at the corners of a square with length L , and each bug moves towards its neighbor at a uniform speed V . This is done in a cyclic fashion, so bug 1 chases bug 2, bug 2 chases bug 3, bug 3 chases bug 4, and bug 4 chases bug 1. Early versions of this problem were described by the popular science writer Martin Gardner, who called it one of *Nine titillating puzzles* [4]. The article asks questions including: “How far does each bug travel before they meet?” In the following month, Gardner showed that the bugs’ trajectories form four congruent logarithmic spirals of length L , that meet at the center of the square at time L/V . Interestingly, the bugs rotate around the center of the square infinitely many times. Gardner uses a geometric argument to calculate the distance travelled, while Watton and Kydon use Calculus [13]. The four bugs problem has been discussed in more recent news media—it appeared in the New York Times’ Numberplay on September 8, 2014. Figure 1(a) shows the logarithmic spirals that each bug follows. The four bugs on a square problem is an example of a general class of problems known as *cyclic pursuit* which dates back to the nineteenth century. A detailed historical description of the problem is provided by Nahin [10].

Researchers have extended the model so that the bugs reach one of two steady states: they either meet at a common point or they enter into a circular cycle. Baryshnikov and Chen [1] use the terminology *rendezvous* and *circular choreography* to mean the case when bugs meet at a mutual point or when they enter into a circular cycle, respectively. In this paper, we use the terminology *coalesce* and *cycle*. Therefore, in the classic four bugs on a square problem, the bugs coalesce. One obvious generalization is to initialize the N bugs on the vertices of a regular N -sided polygon [5], and this results in the bugs coalescing. However, by letting $N \rightarrow \infty$, the bugs remain on a circle, resulting in them cycling. Other generalizations include the introduction of non-linear or deviated steering laws that determine the angular velocity of each bug. This can result in a cycle, and examples of stable paths that the bugs will follow can be circular [9], polygonal [8], or a figure-eight [1]. Another way to produce cycling behavior is to introduce time-dependent speed [2, 6]. Finally, stability of self-similar shapes that the bugs follow when they coalesce has also been analyzed [11].

Another generalization of the classic problem involves initializing the bugs at positions other than the corners of a regular polygon. For example, four bugs can be initialized at the four corners of a 2×1 rectangle [3]. In this case, the bugs’ locations are always the vertices of a parallelogram, and that they meet in the middle at time $1.5L/V$. The bugs coalesce at the middle of the initial rectangle, and do so very

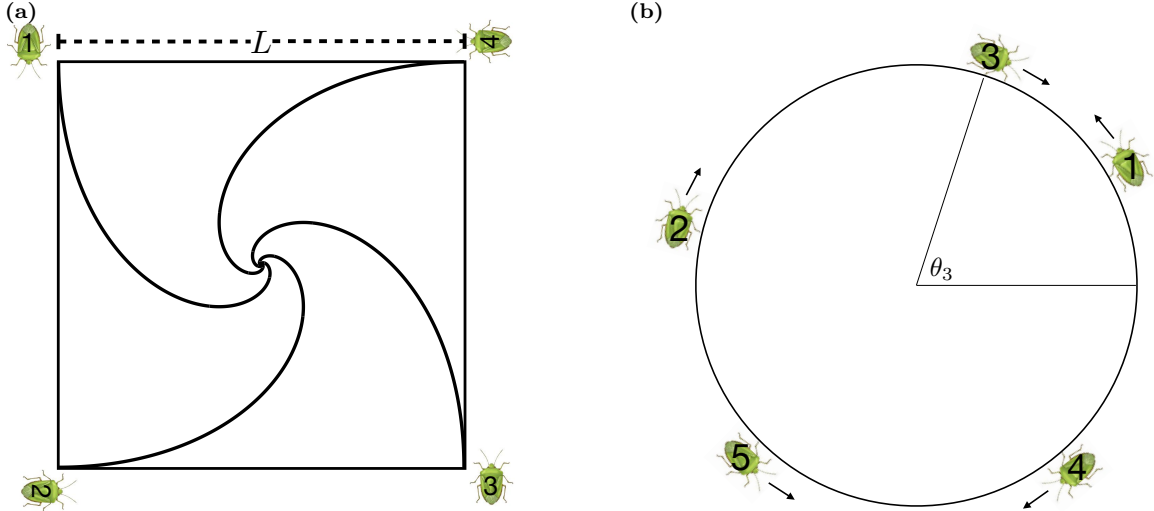


Figure 1: (a) Four bugs placed on the vertices of a square with sides of length L . The trajectories of the bugs are logarithmic spirals of length L that meet at the middle of the square at time L/V . (b) Five bugs chasing each other around a circle. The angle θ_i is the polar angle of bug i . The arrows denote the direction the bugs travel in the current configuration.

rapidly—after each bug has completed one rotation, they again form a 2-1 rectangle, but it has shrunk by a factor of $10^{427907250}$. A broader generalization of cyclic pursuit are evasion problems. These problems often have two groups of agents that are trying to evade another group of agents. Seven Classic Evasion Problems are described by Nahin [10]. For example, in the “Princess-and-Monster Game”, two agents are moving at discrete points along the perimeter of a circle, but they are unaware of one another’s moves. This problem relates to ours, which we describe next, since the agents are constrained to the perimeter of the circle.

In this work, we initialize N bugs on the perimeter of the unit circle, and require the bugs to only move in the tangential direction with uniform speed. Interpreting each bug’s location as a point on the unit circle in the complex plane, the N bugs at time t are located at $z_j(t) = e^{i\theta_j(t)}$, $\theta_j \in [0, 2\pi)$, $j = 1, \dots, N$. As in the case of a cyclic pursuit problem, each bug moves toward its neighbor in a cyclic fashion, but the motion is restricted to the angular direction at a constant angular velocity. We assume that each bug can always see its neighboring bug across the circle, thereby allowing it to know whether to move clockwise or counterclockwise. If bug i and bug $i + 1$ meet, then they form a cluster and collectively chase bug $i + 2$. However, if bugs i and j meet, with $|i - j| \neq 1$, then they simply pass through one another and continue to chase bugs $i + 1$ and $j + 1$, respectively. Figure 1(b) shows a configuration of $N = 5$ bugs, and the direction that each bug is currently traveling. Given this current configuration, bugs 1 and 2 will eventually cluster and pursue bug 3, and bugs 4 and 5 will eventually cluster and chase bug 1.

Just like in the classic problem, the bugs can coalesce to a single point. The inevitable coalescence of all bugs to a single point can be detected if, at any point in time, all bugs are located on one side of a diameter of the circle (Figure 2(a)). However, a major difference introduced by this generalization is the existence of additional steady states without requiring any other generalizations of the problem. First, two groups of bugs can be located at antipodal points on the circle (Figure 2(b)). This configuration results in the bugs not moving, but it is an unstable steady state. Any perturbation to the bugs results in the system tending to another steady state. Second, the bugs can be distributed around the circle so that they are all moving in the same direction. This results in a cycle where the bugs continuously move, but never reach one another (Figure 2(c)). This configuration can be easily detected if at any point in time, all the bugs are moving in the same direction.

In this paper, we analyze these steady states by considering their stability, and calculating probabilities that randomly initialized bugs reach one of these states. Section 2 introduces the notation and governing equations. Section 3 analyzes stability and probabilities analytically for the case $N \leq 4$. Then Section 4 describes a numerical method to simulate the bugs’ dynamics and uses Monte Carlo methods to study the

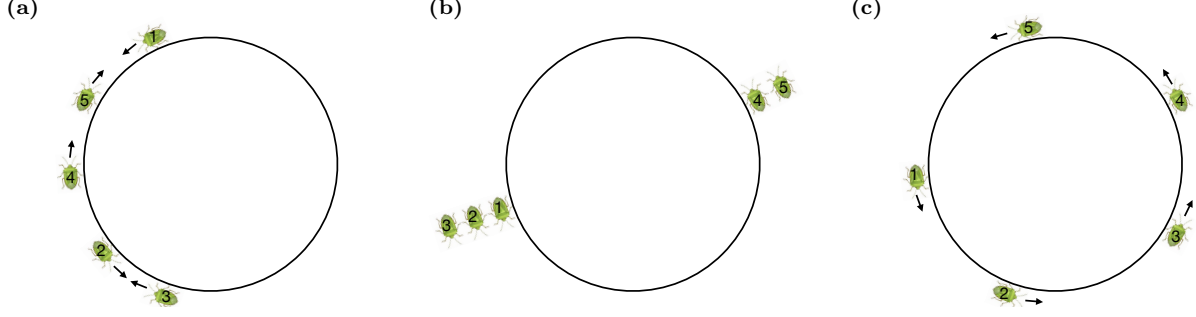


Figure 2: *Three possible steady states. (a) All the bugs are located on the same side of a diameter of the circle. The bugs will eventually coalesce at a single point which is a stable steady state. (b) Groups of bugs are located directly across from one another. This steady state is unstable. (c) Each bug is moving in a counterclockwise direction, resulting in a cycle. This steady state is stable.*

stability and probabilities for large numbers of bugs.

2 Governing Equations and Notation

Given bugs located at locations $z_j(t) = \exp(i\theta_j(t))$, $j = 1, \dots, N$, bug j is governed by the equation

$$\frac{d}{dt}\theta_j(t) = \begin{cases} +1, & \text{mod } (\theta_{j+1} - \theta_j, 2\pi) \in (0, \pi), \\ -1, & \text{mod } (\theta_{j+1} - \theta_j, 2\pi) \in (\pi, 2\pi), \\ 0, & \text{mod } (\theta_{j+1} - \theta_j, 2\pi) \in \{0, \pi\}. \end{cases} \quad (1)$$

Since we assume cyclic pursuit, we associate bug $(N+1)$ with bug 1. It is convenient to maintain each bug's angle within the interval $[0, 2\pi)$. Therefore, if a bug passes through the point $(1, 0)$ (i.e. $\theta_j = 0$), then we either subtract or add 2π to the angle. For simplicity, we omit the mod notation throughout, but note that we consider all angles to be defined in the principal branch $[0, 2\pi)$.

Our model is closely related to the Kuramoto model [7]

$$\dot{\theta}_j = \omega_j + \sum_{k \neq j} K_{jk} \Phi(\theta_j - \theta_k), \quad (2)$$

which is used to describe synchronization of chemical and biological oscillators. Equation (1) reduces to equation (2) when $\omega_j = 0$, $\Phi(z) = z$, and

$$K_{jk} = \begin{cases} 1, & j = k + 1, \\ 0, & \text{otherwise.} \end{cases} \quad (3)$$

While Kuramoto models can exhibit chaos for sufficiently large N , chaos is not expected for solutions to (1). Although, as we will see, it can take a long time before the system converges to a steady state.

To study the stability of equation (1), it is sometimes convenient to decrease the number of unknowns from N to $N - 1$ by arbitrarily rotating the whole system at each time so that bug 1 is always located at $\theta_1 = 0$. We introduce the variables

$$\omega_j = \theta_{j+1} - \theta_j, \quad j = 1, \dots, N - 1, \quad (4)$$

which measures the angle between neighboring bugs. The governing equations for the angle ω_j depend on the relative location of θ_{j+1} and θ_j , and the relative location of θ_j and θ_{j-1} . In particular

$$\frac{d}{dt}\omega_j(t) = \begin{cases} +2, & \omega_{j+1} \in (0, \pi), \text{ and } \omega_j \in (\pi, 2\pi), \\ -2, & \omega_{j+1} \in (\pi, 2\pi), \text{ and } \omega_j \in (0, \pi), \\ 0, & \text{otherwise.} \end{cases} \quad (5)$$

The case $\dot{\omega}_j(t) = 0$ occurs when both bugs j and $j + 1$ are moving in the same direction.

In addition to studying the problem's dynamics, we consider the problem from a statistical point of view. Under a random initialization of the N bug locations, the system evolves to one of three states: $X_N = \text{coalesce}$ (Figure 2(a)), $X_N = \text{groups}$ (Figure 2(b)), or $X_N = \text{cycle}$ (Figure 2(c)). As mentioned earlier, the **groups** steady state is unstable, meaning that N randomly initialized bugs reach this state is with probability 0. Therefore, X_N is a binary random variable that takes on one of the two values

$$X_N = \{\text{coalesce}, \text{cycle}\}. \quad (6)$$

We define p_N as the probability that N randomly initialized bugs reach a **cycle** state, and then $1 - p_N$ is the probability that N randomly initialized bugs reach a **coalesce** state. One of the main goals of this paper is to calculate p_N for small N and estimate p_N using Monte Carlo methods for large N .

3 Analytic Calculations for Small N

For sufficiently small N , the stability of the steady states, and probabilities that randomly initialized bugs reach such a state can be calculated analytically. In this section, we consider the cases $N = 2, 3$, and 4.

3.1 Two Bug Case

Although trivial, it is insightful to first consider the two-bug case. The governing equation for $\omega = \theta_2 - \theta_1$ is

$$\frac{d\omega}{dt} = f(\omega) = \begin{cases} -2, & \omega \in (0, \pi), \\ +2, & \omega \in (\pi, 2\pi), \\ 0, & \text{otherwise.} \end{cases} \quad (7)$$

The two fixed points are clearly $\omega = 0$ and $\omega = \pi$ which correspond to the cases $\theta_1 = \theta_2$ and $\theta_2 - \theta_1 = \pi$, respectively. We analyze the stability of each of these fixed points by considering small perturbations. Letting $\epsilon > 0$, we have that $f(0 + \epsilon) < 0$ and $f(0 - \epsilon) > 0$, showing that the system will return towards 0 under a small perturbation, rendering $\omega = 0$ a stable steady state. Conversely, $f(\pi + \epsilon) > 0$ and $f(\pi - \epsilon) < 0$, showing that the system will diverge from π under a small perturbation, rendering $\omega = \pi$ an unstable steady state. Alternatively, we can analyze the stability of each of these steady states by noting that

$$f'(\omega) = 4\delta(\omega - \pi) - 4\delta(\omega - 0), \quad (8)$$

where we have taken the derivative in the weak sense, and δ is the Dirac delta function. With a slight abuse of notation, we see that $f'(\pi) > 0$ and $f'(0) < 0$, showing that the $\omega = \pi$ is an unstable fixed point while $\omega = 0$ is a stable fixed point. Even without this analysis, the stability is intuitively clear since the case $\omega = \pi$ corresponds to bugs being antipodal to one another, and any small perturbation would result in the bugs moving towards the stable fixed point $\omega = 0$, the case where the bugs are at the same location. In conclusion, given an initial condition of the bug locations, we have that the bugs will always coalesce, meaning that

$$p_2 = 0. \quad (9)$$

3.2 Three Bug Case

The $N = 3$ case introduces interesting behaviors that are absent in the $N = 2$ case. We first write the governing equations in terms of $\omega_1 = \theta_2 - \theta_1$ and $\omega_2 = \theta_3 - \theta_2$. To see that there is a stable cycle steady state, meaning that $p_3 > 0$, suppose that the bugs are initialized at $\theta_1 = 0$, $\theta_2 = 2\pi/3$ and $\theta_3 = 4\pi/3$. In this case, $\omega_1 = \omega_2 = 2\pi/3$. Since $\omega_1 \in (0, \pi)$ and $\omega_2 \in (0, \pi)$, equation (5) shows that $\dot{\omega}_1 = \dot{\omega}_2 = 0$, meaning that the pairwise distances do not change. In this configuration, all three bugs rotate counterclockwise at a uniform speed. Furthermore, under a sufficiently small perturbation of the bug locations, we will still have $\dot{\omega}_1 = \dot{\omega}_2 = 0$, meaning that this steady state is stable. Finally, to confirm that the bugs can still **coalesce**, meaning that $p_3 < 1$, recall that if all bugs are located on one side of any diameter of the circle, then they will **coalesce**.

The $N = 3$ case is sufficiently simple that p_3 can be calculated analytically. We calculate the probability that the bugs enter the **cycle** steady state and rotate counterclockwise. We can perform this calculation in terms of ω_1 and ω_2 , but it is convenient to use the variables θ_1 , θ_2 , and θ_3 . The system can reach this steady state only if the bugs are initialized so that they are all moving counterclockwise at $t = 0$. Furthermore, because the system is invariant to rotation, we can assume that $\theta_1 = 0$. Therefore,

$$P(X_3 = \text{cycle and counterclockwise}) = P((\theta_2 \in (0, \pi)) \cap (\theta_3 \in (\pi, \theta_2 + \pi))) \quad (10)$$

$$= \left(\frac{1}{2\pi}\right)^2 \int_0^\pi \int_\pi^{\theta_2+\pi} d\theta_3 d\theta_2 = \frac{1}{8}. \quad (11)$$

Doubling the result to account for clockwise rotation, we have that

$$p_3 = \frac{1}{4}. \quad (12)$$

We gain further insight by using a geometric argument by visualizing a phase portrait. Figure 3 shows all possible configurations of the system in terms of $(\omega_1, \omega_2) \in [0, 2\pi)^2$. The vectors show the trajectory that ω_1 and ω_2 will follow towards the steady states. If (ω_1, ω_2) are located in one of the gray triangles, the bugs **cycle** either clockwise (upper right triangle) or counterclockwise (lower left triangle). The unstable **groups** steady states are located at the open black circles, and the stable **coalesce** steady state is at the closed black circle. Points between the open circles ($\omega_1 = \pi$ and $\omega_2 = \pi$) correspond to an unstable **cycle** steady state. Finally, the bugs reach a stable **coalesce** steady state if (ω_1, ω_2) is located interior to a white triangle, if $\omega_1 = 0$, or if $\omega_2 = 0$. We can easily verify that the probability in equation (12) is correct by noting that the area of the gray region comprises one quarter of the total area of the square.

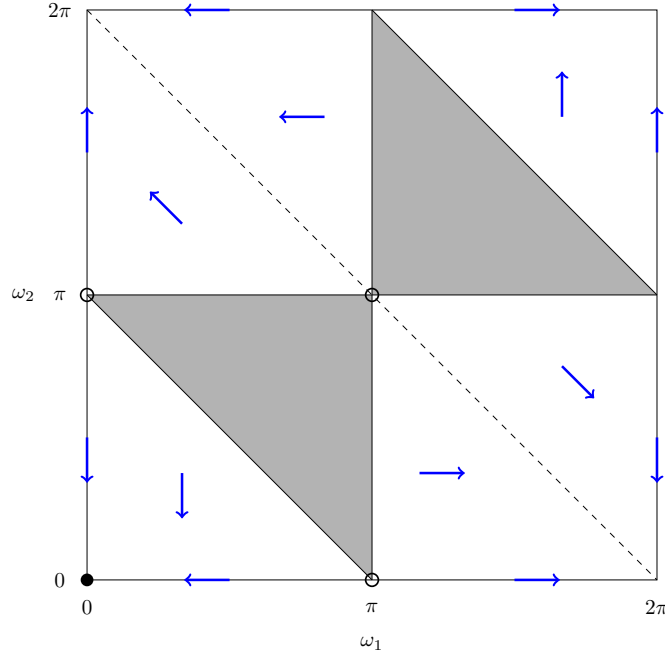


Figure 3: The phase portrait of the $N = 3$ case. The blue arrows show the trajectory of (ω_1, ω_2) . The bugs **cycle** if (ω_1, ω_2) is located in the gray regions. The stable **coalesce** point (filled black point) is $(0, 0)$. The unstable **groups** points (open black points) are $(0, \pi)$, (π, π) , and $(\pi, 0)$. The dashed black line separates regions where both ω_1 and ω_2 are changing, versus where ω_1 is changing while ω_2 is not. Note that the figure is doubly-periodic.

We can use the phase portrait to analyze the instability of the **groups** steady state (open circles). All three of these points have the same stability behavior, so we focus on $(\omega_1, \omega_2) = (\pi, \pi)$, corresponding to

bugs initialized at $\theta_1 = 0$, $\theta_2 = \pi$, and $\theta_3 = 0$. Under a perturbation, we see that the system may enter into the gray region, in which case the bugs will **cycle**, or into the white region, in which case the bugs will **coalesce**. Suppose we allow both ω_1 and ω_2 to be perturbed by $0 < \Delta\omega < \alpha$ (Figure 4). If $\alpha \leq \pi/2$, then the probability that the perturbed system goes to a **cycle** steady state is 0.5. If $\alpha > \pi/2$, then the probability that the perturbed system enters a **cycle** steady state is the area of the gray region inside the red square. A geometric calculation shows that

$$p_3^{\text{stab}}(\alpha) := P(X_3 = \text{cycle} \mid \Delta\omega < \alpha) = \begin{cases} \frac{1}{2}, & \text{if } \alpha \leq \frac{\pi}{2}, \\ \frac{1}{4} \left(-\left(\frac{\pi}{\alpha}\right)^2 + 4\left(\frac{\pi}{\alpha}\right) - 2 \right), & \text{if } \alpha > \frac{\pi}{2}. \end{cases} \quad (13)$$

This result is used to validate our Monte Carlo approach in Section 4.

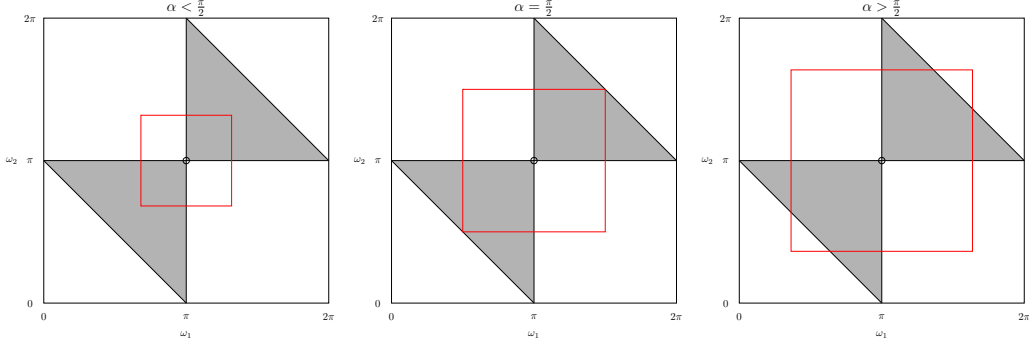


Figure 4: While the fixed point of $(\omega_1, \omega_2) = (\pi, \pi)$ is unstable, small perturbations can result in either a **coalesce** or **cycle** steady state. The probabilities of entering the **cycle** steady state is the area of the gray region inside the red square relative to the area of the red square. The probability is given in equation (13).

3.3 Four Bug Case

We calculate p_4 as a final analytical case before resorting to Monte Carlo methods. As before, we let $\theta_1(0) = 0$. We also make use of symmetry by first assuming that $\theta_2 \in (0, \pi)$, and then doubling the result to calculate p_4 . To determine if a choice for θ_3 and θ_4 will result in a **cycle** or a **coalesce** steady state, we consider four regions of the circle that are defined by the choice of θ_2 . The regions are $(0, \theta_2)$, (θ_2, π) , $(\pi, \theta_2 + \pi)$, and $(\theta_2 + \pi, 2\pi)$. Figure 5 shows these four possible regions that bug 3 can be initialized.

Each possible value for $\theta_3(0)$ defines six intervals. The interval that contains $\theta_4(0)$ determines whether the bugs will reach a **cycle** or **coalesce** steady state. It is obvious in several of the cases if the bugs will **cycle** or **coalesce**. For example, with the configuration in Figure 5(a), if bug 4 is located in $(0, \theta_3)$, then all bugs are initially on the upper hemisphere of the circle, so they will **coalesce**. In contrast, in Figure 5(c), if bug 4 is located in $(\theta_3, \theta_2 + \pi)$, then the four bugs will **cycle**. In each of the four cases for the initial placement of θ_3 , and each of the six cases for the initial placement of θ_4 , the bugs will eventually **cycle** if

- $\theta_3 \in (0, \theta_2)$ and $\theta_4 \in (\pi, \theta_3 + \pi)$;
- $\theta_3 \in (\theta_2, \pi)$ and $\theta_4 \in (\pi, \theta_3 + \pi)$;
- $\theta_3 \in (\pi, \theta_2 + \pi)$ and $\theta_4 \in (\pi, \theta_3 + \pi)$;
- $\theta_3 \in (\theta_2 + \pi, 2\pi)$ and $\theta_4 \in (\theta_3 - \pi, \pi)$.

We can then compute the probability that the four bugs enter a **cycle** state and $\theta_2 \in (0, \pi)$, by integrating

$$P(X_4 = \text{cycle} \cap \theta_2 \in (0, \pi)) = \frac{1}{(2\pi)^3} \int_0^\pi \left(\int_0^{\theta_2} \int_\pi^{\theta_3+\pi} d\theta_4 d\theta_3 + \int_{\theta_2}^\pi \int_\pi^{\theta_3+\pi} d\theta_4 d\theta_3 + \right. \\ \left. \int_\pi^{\theta_2+\pi} \int_\pi^{\theta_3+\pi} d\theta_4 d\theta_3 + \int_{\theta_2+\pi}^{2\pi} \int_{\theta_3-\pi}^\pi d\theta_4 d\theta_3 \right) d\theta_2 = \frac{1}{6}. \quad (14)$$

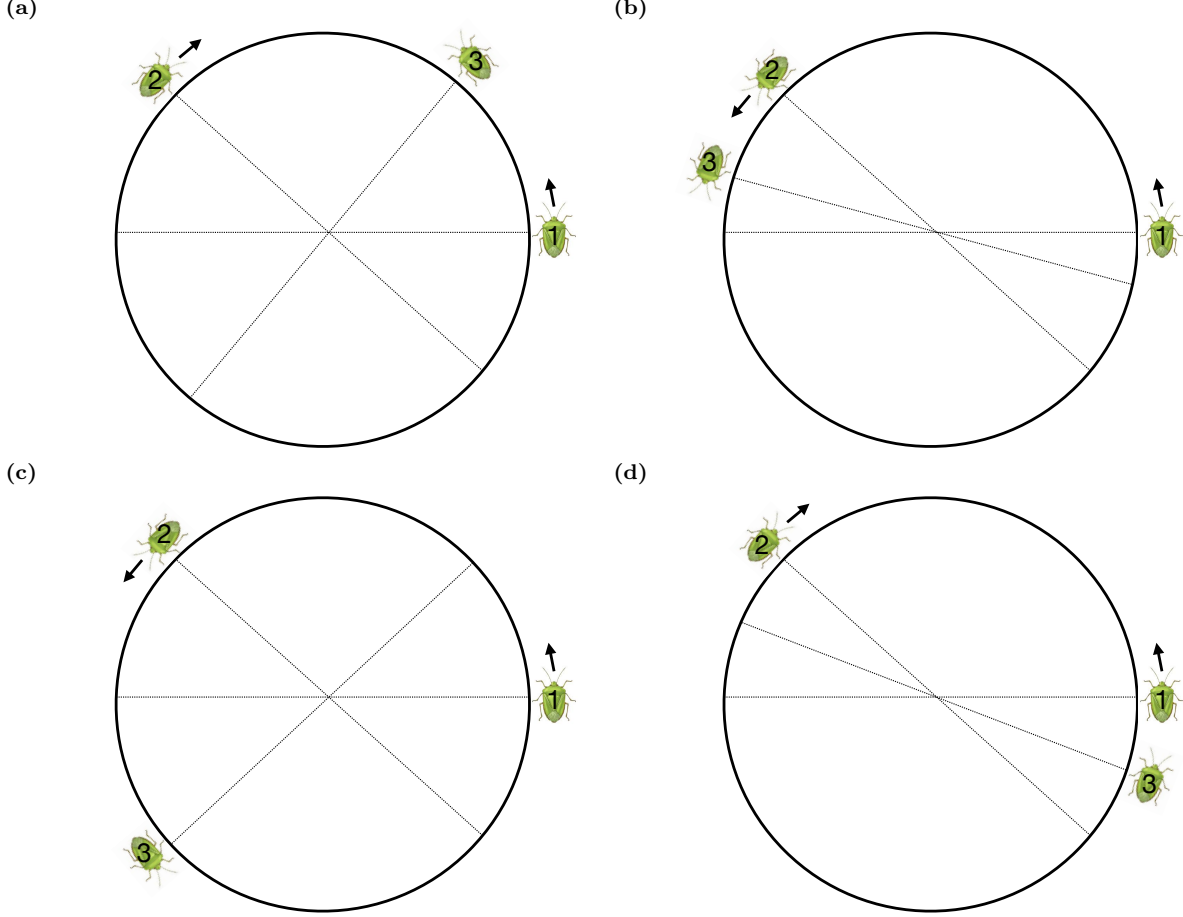


Figure 5: *Four possible initial conditions of bugs 1, 2, and 3 of a four bug system. We assume $\theta_1(0) = 0$ and $\theta_2(0) \in (0, \pi)$. Bug 3 is located in the interval (a) $(0, \theta_2)$, (b) (θ_2, π) , (c) $(\pi, \theta_2 + \pi)$, (d) $(\theta_2 + \pi, 2\pi)$.*

Doubling this result since we assumed that $\theta_2 \in (0, \pi)$, the probability that the four bug system reaches a `cycle` steady state is

$$p_4 = \frac{1}{3}. \quad (15)$$

In summary, for $N \leq 4$, the probability that N bugs reach a `cycle` steady state is

$$p_2 = 0, \quad p_3 = \frac{1}{4}, \quad p_4 = \frac{1}{3}. \quad (16)$$

4 Monte Carlo Simulations for Large N

The analytic approach in section 3 quickly becomes impractical as the number of bugs, N , increases. Therefore, we resort to Monte Carlo methods to estimate the probability that N randomly initialized bugs will enter the `coalesce` or `cycle` state. In particular, we run M experiments that initialize N bugs with the first bug located at $\theta_1 = 0$, while the other $N - 1$ bugs are sampled randomly from $(0, 2\pi)$ with uniform distribution. Once the bugs are initialized, their dynamics are simulated by applying Forward Euler to the governing equation (1). We initially used a time step size of $\Delta t = 0.1$, but found that for larger values of N , two bugs would often end up changing locations back and forth, or a bug would pass more than one bug in a single time step, both of which are unphysical in the continuous limit. We found that by taking $\Delta t < \pi/N$,

these unphysical dynamics are avoided, and the bugs either enter the `cycle` or `coalesce` state. Since we consider at most $N = 100$ bugs, we use the time step size $\Delta t = 0.01$ for all simulations.

Since we only need to determine whether the bugs `coalesce` or `cycle`, we run each simulation until we can determine which state the system will inevitably reach. As described in the introduction, this is accomplished by periodically checking if

- all bugs are traveling in the same direction; or,
- all bugs are on the same side of any diameter of the circle.

The first case is easy to detect since it only requires that the right-hand side of (1) is identically $+1$ or identically -1 . It is slightly harder to detect if the system has entered the second case. In our implementation, we consider the diameters going through each of the N bugs, and if all other bugs lie on the same side of any one of these diameters, then the bugs will inevitably `coalesce`. Figure 6 shows a configuration when a simulation could be stopped since it is inevitable that the bugs will `coalesce`.

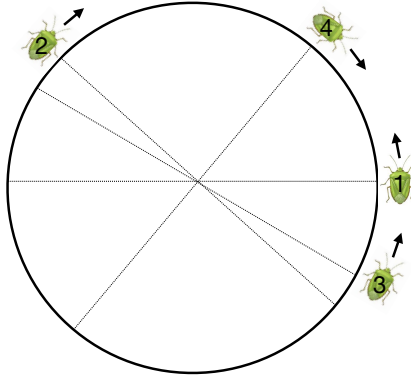


Figure 6: In this configuration, it is clear that the bugs will `coalesce` since all bugs lie on the same side of the diameter passing through bug 2 (and bug 3).

We begin by validating our code against the analytical result for the stability of three bugs initialized at $\theta_1 = \theta_3 = 0$ and $\theta_2 = \pi$. This initial condition corresponds to the open black circle in the center of Figure 4, and the probability that a perturbation no larger than α will `cycle` is given by equation (13). We run M trials for 20 values of α that are uniformly spaced in $(0, \pi)$. When $\alpha = \pi$, perturbations of bugs 2 and 3 can lie anywhere on the unit circle. Performing M simulations provides an estimate $\hat{p}_3^{\text{stab}}(\alpha)$ of equation (13). By the Central Limit Theorem, the error in the estimate follows a normal distribution with a mean of 0 and a variance of

$$\sigma^2 = \frac{\hat{p}_3^{\text{stab}}(\alpha)(1 - \hat{p}_3^{\text{stab}}(\alpha))}{M}. \quad (17)$$

Figure 7 shows the analytical probability (solid line) and the estimated probability using the Monte Carlo approach (error bars) for two different values of M . The error bars are the 95% confidence interval. We observe good agreement between the estimate and exact value of $p_3^{\text{stab}}(\alpha)$, indicating that our numerical approach is appropriate for estimating p_N for larger N .

Having validated that the Monte Carlo approach converges to an analytic result, we now estimate the probability $P(X_N = \text{coalesce}) = 1 - p_N$ for $N = 2, 4, 6, \dots, 100$. Figure 8 shows the result from running $M = 10,000$ samples for each value of N . First, we point out that the Monte Carlo method provides the estimates

$$1 - \hat{p}_2 = 1.00, \text{ and } 1 - \hat{p}^4 = 0.661, \quad (18)$$

which agree with the exact values in equation (16). Next, the left plot of Figure 8 indicates that there is a linear relationship between $\log p_N$ and $\log N$. This indicates a power-law relationship $P(X_N = \text{coalesce}) =$

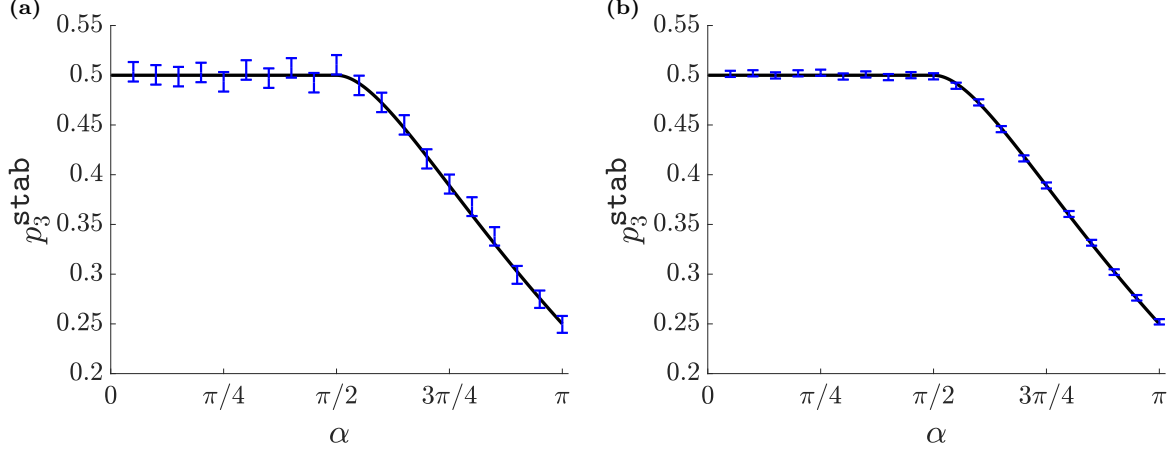


Figure 7: *Validation of the Monte Carlo method. The black curve is the exact probability that a perturbation of size no more than α will enter a **cycle** steady state (equation (13)). The error bars are the 95% error bars of the Monte Carlo estimate using (a) $M = 10^4$ simulations, and (b) $M = 10^5$ simulations.*

aN^p . Using least squares regression, the best fit is

$$P(X_N = \text{coalesce}) \approx 1.33N^{-0.49}, \quad (19)$$

indicating that the probability of coalescing is inversely proportional to the square root of the number of bugs. The right plot of Figure 8 shows the least squares fit (19) (solid line) and the 95% confidence of the Monte Carlo method. While we see that the fit underestimates the Monte Carlo estimate, the difference is slight, indicating that equation (19) provides a good estimate of the probability that N randomly initialized bugs will eventually **coalesce**.

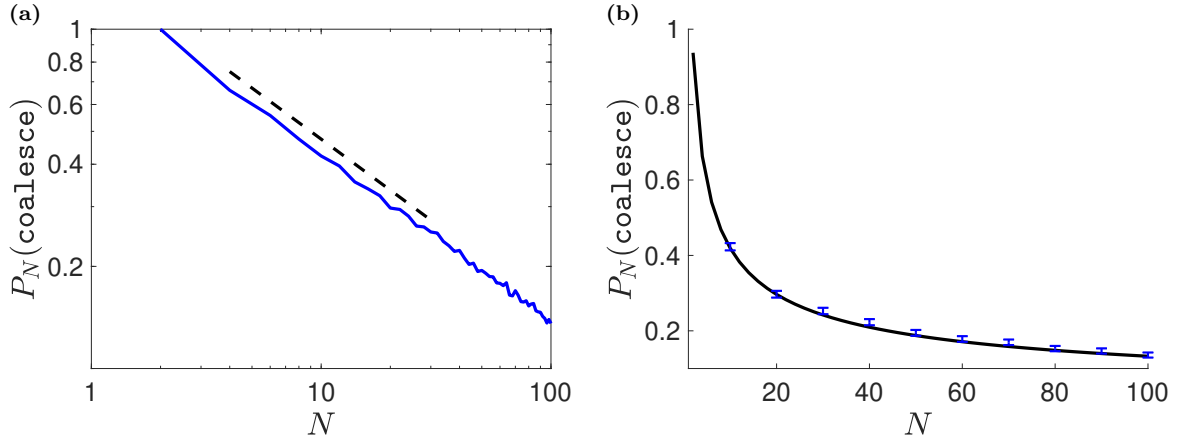


Figure 8: (a) *The estimate \hat{p}_N as function of N . The black dashed line has slope -0.5 and indicates that \hat{p}_N is inversely proportional to \sqrt{N}* (b) *The least squares fit (19) of the probability of the bugs entering a **coalesce** (solid line), and the 95% confidence interval from the Monte Carlo method (intervals).*

5 Order Parameter and Phase Angle

The bug configuration can be characterized using Kuramoto's order parameter and phase angle [7]. The time-dependent order parameter, $r \in [0, 1]$, and the phase angle, $\psi \in [0, 2\pi)$, satisfy

$$re^{i\psi} = \frac{1}{N} \sum_{j=1}^N e^{i\theta_j}. \quad (20)$$

A value of $r = 1$ corresponds to perfect positional order, while $r = 0$ corresponds to complete incoherence. If the bugs **coalesce** at $e^{i\theta}$, then they are perfectly ordered with $r = 1$, and the phase angle is $\psi = \theta$. In contrast, if the bugs cycle clockwise (counterclockwise), then ψ decreases (increases) linearly modulo 2π , and the order parameter r remains constant. The constant equals 0 if the cycling bugs are equally distributed, and it approaches 1 as the bugs begin to cluster. Therefore, the order parameter and phase angle provide an alternative method to determine if N bugs **coalesce** or **cycle**.

Figure 9 shows the order parameter and the phase angle for $N = 100$ bugs that eventually **coalesce**. The bug locations (red dots) are shown at six critical points of the order parameter. The values of r and ψ are denoted by the black line with the black dot. We see that the order parameter can oscillate between maximum and minimum values before ultimately reaching a value of $r = 1$, implying a **coalesce** steady state. Figure 10 shows the order parameter and phase angle of $N = 100$ bugs that eventually **cycle**. Again, the order parameter oscillates between maximum and minimum values before ultimately reaching a value of $r < 1$, implying a **cycle** steady state.

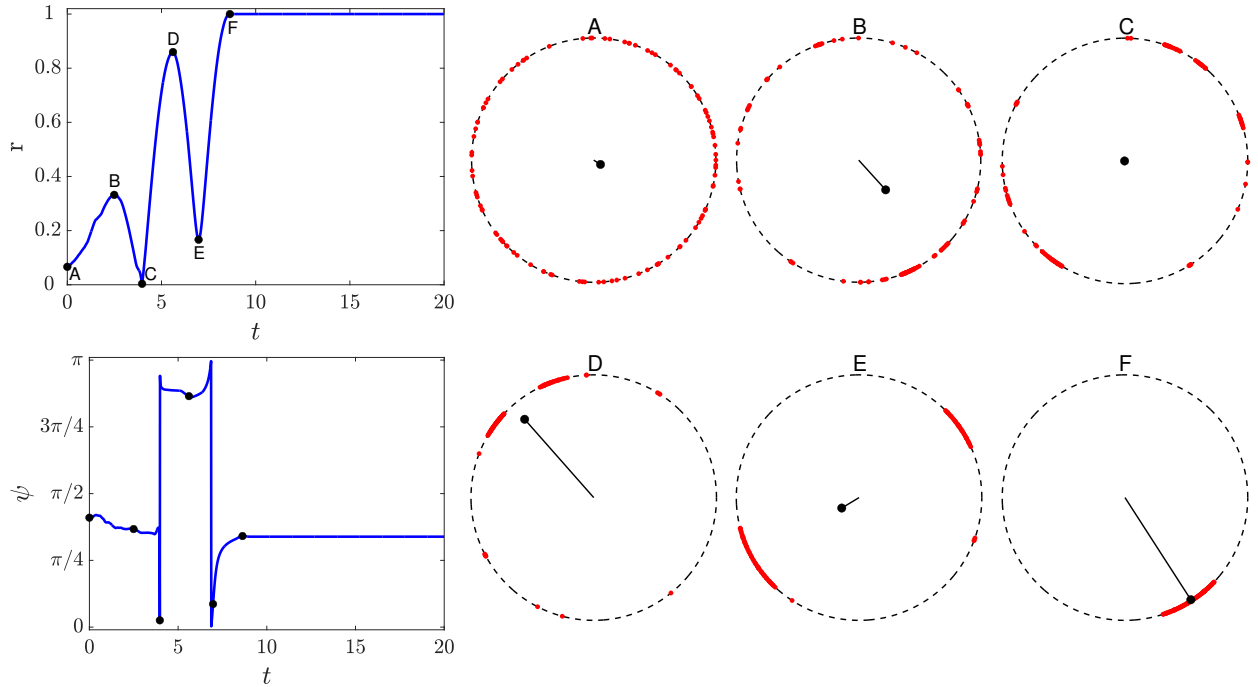


Figure 9: The order parameter, r , and phase angle, ψ , of $N = 100$ bugs that eventually **coalesce**. The bug locations corresponding to the six black marks on the plot of the order parameter are shown. The vector at the center of the circle represents $re^{i\psi}$. Because the bugs **coalesce**, r converges to 1 and ψ converges to a constant.

6 Conclusions

In this work, we investigated a novel generalization of the classic cyclic pursuit problem by constraining the bugs to move exclusively along the perimeter of a unit circle. This geometric restriction changes the system's

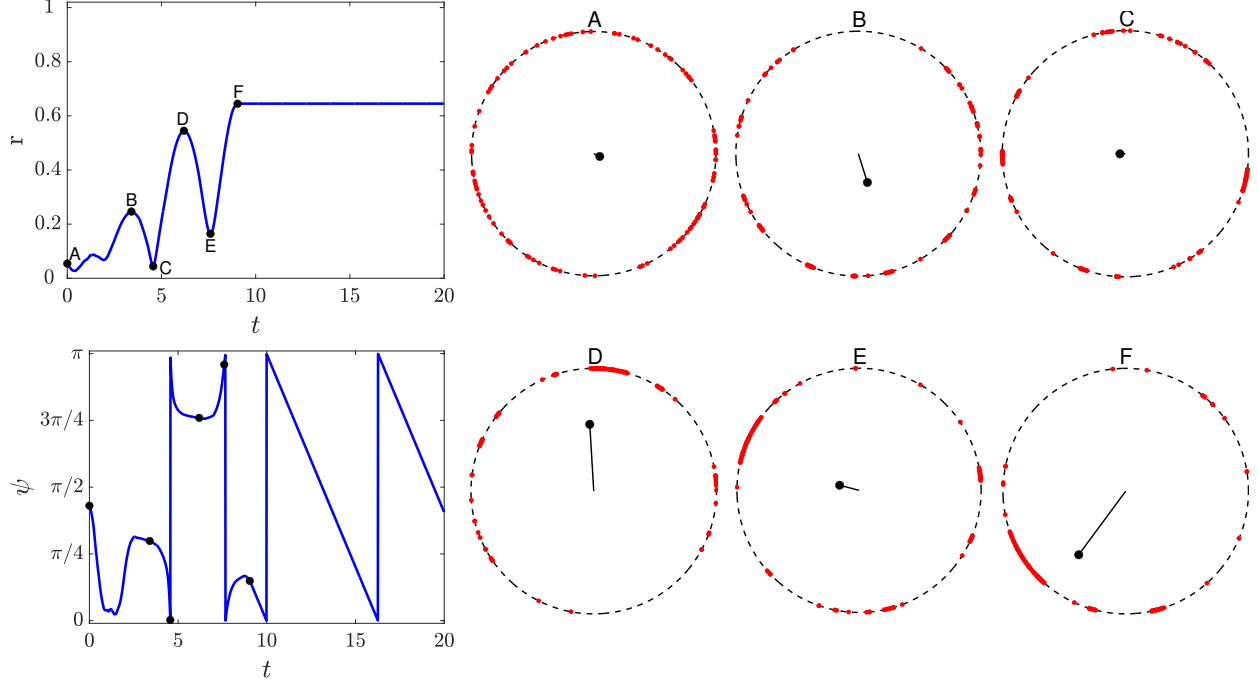


Figure 10: The order parameter, r , and phase angle, ψ , of $N = 100$ bugs that eventually **cycle**. The bug locations corresponding to the six black marks on the plot of the order parameter are shown. The vector at the center of the circle represents $re^{i\psi}$. Because the bugs **cycle** clockwise, r converges to a value less than 1 and ψ decreases linearly with time modulo 2π .

long-term behavior. We identified three possible outcomes: a stable state where all the bugs meet, defined as **coalesce**, a stable state where all bugs infinitely chase one another, defined as **cycle**, and an unstable state where groups of bugs are at antipodal points of the circle, defined as **groups**.

For small numbers of bugs ($N \leq 4$), we derived exact analytical expressions for the probability of entering the **cycle** steady state. These results showed that the probability of cycling increases with N : $p_2 = 0$, $p_3 = 1/4$, and $p_4 = 1/3$. For larger systems, we employed a validated Monte Carlo method to estimate the probability that the bugs will **coalesce**. Our simulations reveal that this probability approximately follows an inverse square-root law,

$$P(X_N = \text{coalesce}) \approx \frac{1.33}{\sqrt{N}}. \quad (21)$$

The dynamics observed in this generalized setting underscore how geometric constraints can lead to qualitatively different collective behavior in pursuit problems.

This study establishes groundwork for several future directions. Future work will focus on a generalization to non-uniform bug speeds. We plan to investigate the behavior of the system if one bug is faster than the others. We conjecture that the bugs will always **coalesce** under this change, but this has not been explored. Additionally, there are a variety of other statistical quantities that can be calculated analytically for small N , and estimated with a Monte Carlo approach for large N . For example:

- What is the minimum expected wait time for N randomly initialized bugs to enter into a stable steady state, where it is clear that they will either **coalesce** or **cycle** based on the conditions established in section 4.
- For large N , non-consecutive bugs can cross one another many times before they enter into the **coalesce** or **cycle** steady state. What is the distribution of the number of crossings?

- For large N , the bugs can enter a **cycle** steady state in which each bug is moving in the same direction, but their position along the circle does not align with the order of their index. In this case, the sequence of indices wraps around the circle more than once, resulting in a winding number greater than one. Figure 11(a) shows $N = 5$ bugs in a **cycle** steady state whose sequence of indices results in a winding number of two. For a given N and an initial condition that results in the bugs reaching a **cycle** steady state, what is the resulting distribution of the winding number?

We are also considering the dynamics of N randomly initialized bugs on two-dimensional manifolds. Others have studied the dynamics of bugs constrained to surfaces of revolution, including a torus [12]. Future directions will also consider bugs on non-orientable surfaces. For example, by placing two bugs on the surface of a transparent Möbius strip embedded in \mathbb{R}^3 , they can be located at the same point while being on “opposite sides” of the surface (Figure 11(b)).

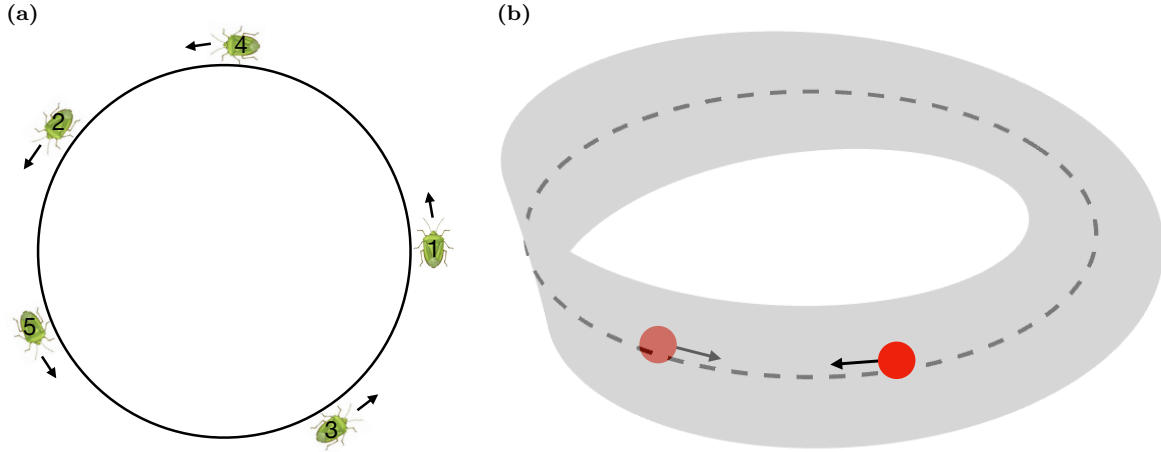


Figure 11: (a) Five bugs in a **cycle** steady state. Note that the indices of the bugs wrap around the circle twice. (b) By interpreting the Möbius strip as a surface in \mathbb{R}^3 with thickness, it is possible for the bugs to reach a steady state where they are on opposite sides of from one another. In this figure, the bugs (red dots) are on “opposite sides” of the Möbius strip.

Acknowledgments: We thank Peter Beerli and Malbor Asllani for their valuable feedback on this paper.

References

- [1] Yuliy Baryshnikov and Cheng Chen. Shapes of Cyclic Pursuit and Their Evolution. In *2016 IEEE 55th Conference on Decision and Control (CDC)*, pages 2561–2566. IEEE, 2016.
- [2] A.M. Bruckstein, N. Cohen, and A. Efrat. Ants, Crickets and Frogs in Cyclic Pursuit. Technical report, Technion-Israel Institute of Technology, Center for Intelligent Systems, 1991.
- [3] S. J. Chapman, James Lottes, and Lloyd N. Trefethen. Four bugs on a rectangle. *Proceedings of the Royal Society A*, 467:881–896, 2011.
- [4] Martin Gardner. Mathematical games. *Scientific American*, 197(5):140–147, 1957.
- [5] Martin Gardner. Mathematical Games. *Scientific American*, 213(1):100–105, 1965.
- [6] M. S. Klamkin and D. J. Newman. Cyclic pursuit or “the three bugs problem”. *The American Mathematical Monthly*, 78(6):631–639, 1971.
- [7] Yoshiki Kuramoto. *Chemical Oscillations, Waves, and Turbulence*. Springer, 1984.

- [8] Joshua A. Marshall, Mireille E. Broucke, and Bruce A. Francis. Formations of vehicles in cyclic pursuit. *IEEE Transactions on Automatic Control*, 49(11):1963–1974, 2004.
- [9] Dwaipayan Mukherjee and Debasish Ghose. Deviated linear cyclic pursuit. *Proceedings of the Royal Society A: Mathematical, Physical and Engineering Sciences*, 471(2184):20150682, 2015.
- [10] Paul J. Nahin. *Chases and escapes: the mathematics of pursuit and evasion*. Princeton University Press, 2012.
- [11] Tom Richardson. Stable polygons of cyclic pursuit. *Annals of Mathematics and Artificial Intelligence*, 31(1):147–172, 2001.
- [12] Francisco J. Solis and Carlos Yebra. Pursuit on regular surfaces with application to consensus problems. *Nonlinear Dynamics*, 105(4):3423–3438, 2021.
- [13] A. Watton and D. W. Kydon. Analytical Aspects of the N-Bug Problem. *American Journal of Physics*, 37(2):220–221, 1969.